NASA TND-1764

33p.

TECHNICAL NOTE

D-1764

A STUDY OF THE HYDROGEN, HELIUM, AND HEAVY NUCLEI IN THE NOVEMBER 12, 1960, SOLAR COSMIC RAY EVENT

S. Biswas, C. E. Fichtel, and D. E. Guss
Goddard Space Flight Center
Greenbelt, Maryland

NATIONAL AERONAUTICS AND SPACE ADMINISTRATION
WASHINGTON
May 1963

Code-1

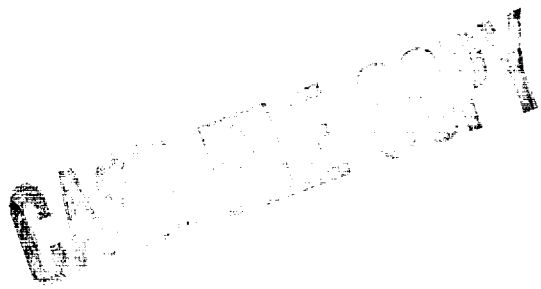

A STUDY OF THE HYDROGEN, HELIUM, AND HEAVY NUCLEI IN THE NOVEMBER 12, 1960, SOLAR COSMIC RAY EVENT

by

S. Biswas, C. E. Fichtel, and D. E. Guss
Goddard Space Flight Center

SUMMARY

The composition and energy spectra of solar cosmic rays from the November 12, 1960, solar flare were studied by using rocket-borne nuclear emulsions. The abundances of hydrogen, helium, carbon, nitrogen, oxygen, neon, and larger nuclei were determined; and upper limits were set for light nuclei ($3 \leq Z \leq 5$) and fluorine nuclei. The relative numbers of helium, light, medium ($6 \leq Z \leq 9$), and large ($Z \leq 10$) nuclei in the solar beam were found to be 680 ± 110, <0.1, 10, and 1.0 ± 0.3 respectively. The composition was similar to that of the solar atmosphere, as determined by spectroscopic means, for those elements where a comparison could be made but was markedly different from that of galactic cosmic rays.

The differential energy per nucleon spectra of hydrogen, helium, and medium nuclei could be represented by an equation of the form $dJ/dW = K(W/W_0)^{-\gamma}$ for kinetic energies greater than 35 Mev/nucleon. The values of γ for helium and medium nuclei were the same within uncertainties, but larger than that for hydrogen nuclei by a factor of more than 2 in the energy interval from 40 to 130 Mev/nucleon. In spite of the different energy per nucleon spectra, the ratio of protons to heavier nuclei in a given energy per nucleon interval was the same at different times in the event and was also the same as that observed in two other events. The measurements are shown to be consistent with a diffusion process having a predominantly velocity dependent diffusion coefficient at low energies, as suggested by Parker; and therefore the different energy per nucleon spectra mentioned earlier are probably due to differences generated by the acceleration process. Present ideas concerning the acceleration mechanism for solar cosmic rays are discussed in relation to the experimental results.

CONTENTS

A STUDY OF THE HYDROGEN, HELIUM, AND HEAVY NUCLEI IN THE NOVEMBER 12, 1960, SOLAR COSMIC RAY EVENT*

by

S. Biswas†, C. E. Fichtel, and D. E. Guss

Goddard Space Flight Center

INTRODUCTION

Many studies have been made of the proton energy spectrum of solar cosmic ray events by means of balloons and satellites. Information on the helium nuclei at balloon altitudes (References 1 and 2) was obtained in several events by the University of Minnesota's nuclear emulsion group. In a NASA sounding rocket firing that was part of the solar cosmic ray experiment at Fort Churchill, Canada, some data on the protons, helium nuclei, and heavy nuclei ($Z \geq 3$) were obtained at one time during the September 3, 1960, event (Reference 3). Although these results gave the first indication of the very gross relative abundances of the heavy nuclei, and the heavy nuclei to proton ratio, the limited statistics did not permit a detailed analysis of the composition or a determination of the energy spectrum of any but the proton component.

Subsequently two similar rocket firings with successful nuclear emulsion recovery were made during the high-intensity solar cosmic ray event of November 12, 1960; in this event there were sufficient numbers of particles to permit a detailed analysis of the helium and heavy nuclei. This paper presents an analysis of the particle properties of the November 12, 1960, event as determined from the nuclear emulsions recovered from the two firings just mentioned.

In particular, the charge composition is studied up to charge 18 for particles with an energy per nucleon in excess of a few 10's of Mev. The energy spectra of the protons, helium nuclei, and medium nuclei ($6 \leq Z \leq 9$) are compared in the same energy intervals and the same rigidity intervals. This new information is discussed in terms of some of the existing theoretical models related to solar cosmic ray events in an attempt to obtain a better understanding of the sun, the acceleration mechanism for these high energy particles, and the interplanetary modulation. Finally, the composition of the solar cosmic rays is compared with that of ordinary galactic cosmic rays to show that there are some very marked differences.

*Also published in: *Physical Review* 128(6):2756-2771, December 15, 1962.

†NASA-National Academy of Sciences Senior Postdoctoral Resident Research Associate; on leave from Tata Institute of Fundamental Research, Bombay, India.

DESCRIPTION OF THE EVENT

The November 12, 1960, event was one of the largest ever recorded. The total integrated particle flux for this event is estimated to be about 2×10^8 particles/cm^2-ster for particles with energies greater than 20 Mev. This is almost two orders of magnitude greater than the normal galactic cosmic ray flux for a whole year. Further, the integral energy flux was approximately 3×10^4 ergs/cm^2-ster, which is somewhat larger than that from cosmic rays for 1 year.

The flare considered to be the source of the solar cosmic ray particles that began to reach the earth on November 12, 1960, was preceded by a period of relatively important solar activity. On November 10, 1960, there was a class 3 flare at 1000 UT in the McMath plage region 5925. On November 11, 1960, a major type IV radio noise outburst was observed in Japan and Australia beginning at about 0304 UT. At approximately the same time, Voroshilov observed a major flare that reached a maximum at about 0340 UT. On November 12, 1960, at 1322 UT a class 3 flare occurred; and very shortly thereafter, at 1340 UT, a neutron monitor increase began at Deep River (Reference 4) and other stations. Two magnetic storms followed shortly thereafter, at 1348 and 1844 UT; they are believed to be associated with the major flares of November 10 and 11. Following the second sudden commencement, at 1900 UT there was a second sharp increase in the Deep River neutron monitor counting rate, which, after having increased for 2-1/2 hours, had begun to decline. However, at the same time there was a Forbush decrease on the Massachusetts Institute of Technology meson telescope, indicating that the very high energy galactic cosmic rays were being partially excluded from the region of the earth.

Vogan and Hartz (Reference 5) observed that the 60-Mc riometers showed a sharp increase in absorption at approximately 1900 UT on November 12, 1960. Steljes et al. (Reference 4) have shown that these and other considerations form a solid base for the proposition that the particles from the 1322 UT November 12 flare were at least partially contained within the walls of a "magnetic bottle" formed by the gas cloud associated with the November 11 flare expanding from the sun. There was a considerable leakage from the bottle, as indicated by the increase in particle intensity prior to 1900 UT November 12. The first of the two recovered payloads was fired at 1840 UT, and therefore the information gathered represents a sample of the particle flux just before the effects of the second magnetic storm were felt.

On November 13, 1960, at 1021 UT there was *another* sudden commencement, presumably associated with the November 12 flare, followed by another Forbush decrease at 1035 UT (Reference 4). No appreciable prolonged change was noted in the riometer absorption at this time; this indicated that the second sudden commencement had little effect on at least the low energy component, which according to the riometer was only slightly less than maximum intensity. The second firing of the event of November 12, 1960, from which a payload was recovered occurred at 1603 UT on November 13, and therefore represents a study of this period of near maximum low energy flux.

After this time the particle density – as measured by the riometer and balloon flight at Minnesota – continued to decrease until early on November 15, when another solar cosmic ray event prevented the further study of this event.

A summary of the Deep River Neutron Monitor record (Reference 4), the Fort Churchill riometer data,* and the two rocket flight times is shown in Figure 1.

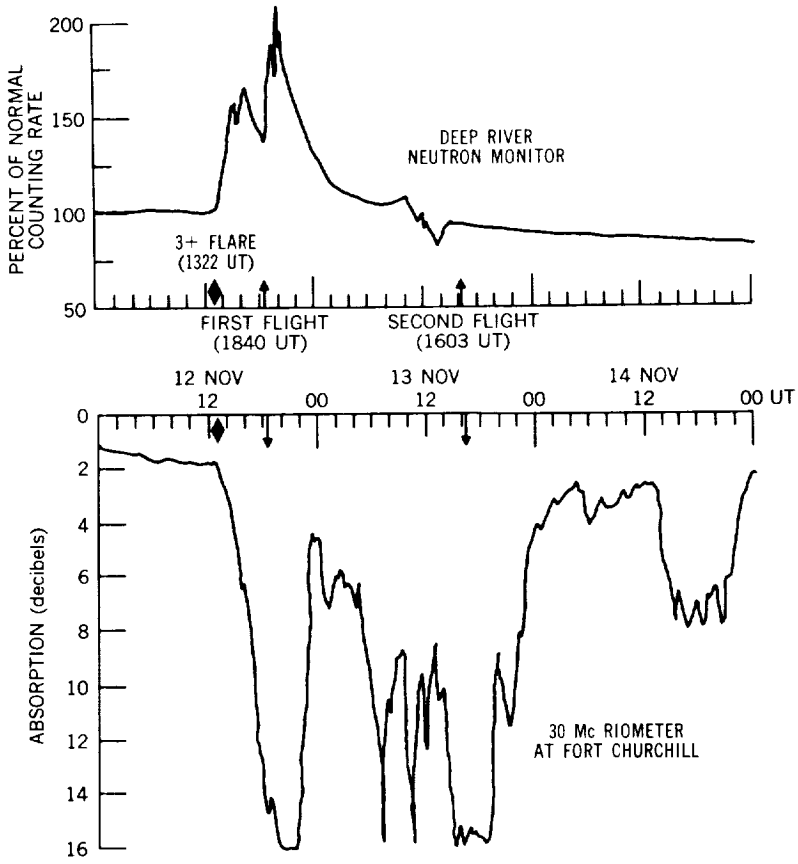

Figure 1 — Deep River neutron monitor record and the Fort Churchill riometer absorption curve. Flight times for the two rockets of this experiment are indicated by arrows. Class 3+ flare began at 1322 UT on Nov. 12, 1960, indicated by solid diamond symbols.

EXPERIMENTAL PROCEDURE

Rocket and Payload System

To study the low energy component of solar cosmic rays and to take advantage of the special properties of nuclear emulsions in order to examine their charge spectrum, research sounding rockets with recoverable payloads were kept on a 24 hour/day standby at Fort Churchill, Canada, from June 6, 1960, until the end of the firings in November 1960. The Nike-Cajun rocket was chosen because: It could be prepared for firing quickly; a number could be kept on a standby for launching into the same event; it could carry the 85-pound payload to a peak altitude of 130 kilometers, permitting a several minute exposure under less than 0.01 gm/cm^2 of atmosphere; it had a recovery system that could be easily modified for these needs; it could be fired from Fort Churchill, where entry of the low energy particles to be studied is not prevented by the earth's magnetic field (References 6, 7, and 8); and it was a proved system.

*Courtesy of Defense Research Telecommunications Establishment, Ottawa, Canada.

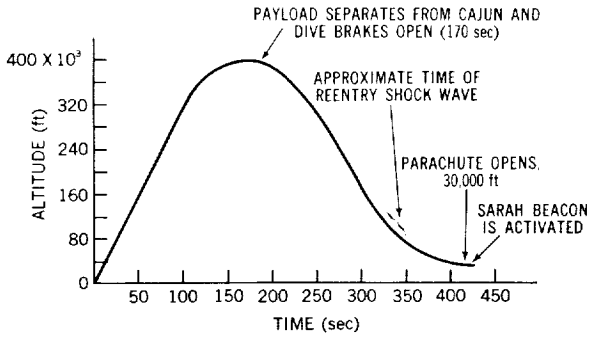

Figure 2—Nike-Cajun trajectory.

The payload* was divided into four parts: a *recovery section*, a *nuclear emulsion section*, an *instrumentation section*, and an *ogive nose-cone*. The *recovery section* included a parachute, a SARAH beacon, dive brakes for reentry stabilization, and dye packages. The sequence of operation of the recovery section is illustrated, along with the Nike-Cajun trajectory, in Figure 2. Successful recovery of the payload depended primarily on homing-in on the SARAH beacon with a helicopter, impact prediction by SOTIM,† and visual sighting – since attempts to track the rocket flights by radar failed. In spite of difficult recovery conditions, two of the three payloads fired into the November 12, 1960, event were recovered.

The *nuclear emulsion section* consisted of: a central cylinder of forty 600μ-thick Ilford G5 nuclear emulsions in the shape of 4-inch-diameter disks whose planes were perpendicular to the rocket axis, four structural posts 90 degrees apart, and an outside cylindrical aluminum skin that was 6-3/4 inches in diameter and 0.024 inch thick. This thickness was the minimum that would withstand the heat and strains of the flight and still maintain a watertight seal. As an additional protection against heat, the emulsions were covered with thin heat-radiation-reflecting aluminum foil. A sheet of 1-mil Mylar was placed between the foil and the emulsions to prevent the aluminum from reacting with the emulsions. The total amount of material between the emulsions and the ambient radiation, once the payload was out of the atmosphere, was then 0.19 gm/cm^2 – largely aluminum.

The *instrumentation section* contained flight performance instruments (including a magnetometer and accelerometer) and electronic counters, the data from which are being published separately (Reference 9).

Proton Component

The emulsions were scanned on specially constructed microscope stages that provided precision rotational motion about the center of the circular emulsion sheet and a radial motion. The scanning was performed in the middle 80 percent of the emulsion thickness at distances of 0.5, 1.3, and 3.5 mm in from the edge for all tracks lying in the solid angle interval defined by $|\alpha| \leq 20$ degrees and $|\beta| \leq 20$ degrees, and at distances 10.00 and 20.0 mm for all tracks in the solid angle interval defined by $|\alpha| \leq 20$ degrees and $|\beta| \leq 10$ degrees. Here α is the angle between the projection of the track on the emulsion plane and the radius vector of the emulsion disk measured at the scan line,

*The payload was constructed by Cook Research Laboratories in accordance with the specifications of the Goddard Space Flight Center.
†A system whereby several sets of microphones on the ground are used to receive the sound produced by reentry of the payload into the atmosphere. An impact point is estimated by triangulation.

and β is the angle of the track with respect to the plane of the emulsion. The usual scanning efficiency checks (Reference 10), such as comparing the distributions of number of tracks found versus α, β, and emulsion depth with the expected distributions and rescanning by a second scanner, were performed. In addition, scans were performed in all four quadrants of the emulsion disks, and the intensity of tracks obtained in each was found to be the same within the statistical uncertainties. This would be expected, since the rocket was known to be spinning rapidly about its axis during the flight.

The scans described above make it possible to derive integral proton intensities in the range of energies between 14.5 and 81 Mev. To extend the spectrum to higher energies, the energies of those particles producing tracks in the scan 10.00 mm in from the edge of the emulsion were determined from ionization measurements, using the Fowler-Perkins method (Reference 11) of the *blob-gap* counting. The tracks were selected for the blob-gap measurement if they had an ionization greater than 1.3 times minimum, as determined from a prior blob count. This was two standard deviations below the ionization corresponding to the highest energy point included in the integral spectrum. Because the spectrum is a steeply falling function of energy in this energy region, the finite resolution of the ionization measurements results in an artificial particle increase toward higher energy; and a shift of the order of 4 percent was made to compensate for this effect.

The results obtained from the scans described above must be corrected for particles *other than solar protons* that are picked up in the scans. These are background tracks collected before and following the flight, galactic cosmic ray protons collected during the flight, and solar helium nuclei. Because of the energy spectrum's shape, the contribution of secondary tracks from interactions in the emulsion is negligible for the range of energies under discussion. The contribution from background tracks was determined from scans in emulsions that were kept with the flight stack at all times except during the rocket flight; and the contribution from galactic cosmic ray particles was determined from scans in the emulsion stack that was flown during a solar "quiet" time. The correction to the particle densities from both of these contributions was less than 1 percent at proton energies less than 120 Mev. At higher energies these corrections became appreciable, and the high energy limit of the spectrum was set at that energy where the expected background contribution was the same order as the sample: 340 Mev in the first flight, and 270 Mev in the second. The contribution of solar helium nuclei was determined as described in the next section, and this correction was made to the proton flux.

To calculate intensities, some assumption must be made about the isotropy of the solar particles. It was assumed that the solar particles during these flights were isotropic over zenith angles $\theta \leq 90$ degrees and zero for zenith angles $\theta \geq 90$ degrees + δ. The particles present between 90 degrees and 90 degrees + δ are those that have mirrored in the magnetic field of the earth below the altitude of the rocket and have returned. The mirrored particles are degraded in energy by ionization loss in the atmosphere while twice traversing the spiral path from the rocket altitude to the mirror point. The angle δ is a function of the ambient proton energy and the rocket altitude; however, even for the highest energy particles considered, δ did not exceed 10 degrees. An analysis of the Geiger counter data on the flights is consistent with these assumptions.

With the above assumption of isotropy, an integral energy spectrum can be constructed from the data that have been corrected for background, galactic cosmic rays, and solar helium nuclei. This

spectrum is a good first approximation to the ambient spectrum and, by using it as a trial spectrum, the true spectrum of solar protons—corrected for rocket trajectory—is obtained by a method of iteration as explained below.

The trajectory correction consists of two parts: (1) those particles collected by the emulsion in its ascent and descent through the atmosphere, and (2) those particles collected when the rocket is above the atmosphere. The particles in (1) are degraded in energy by ionization loss in the atmosphere above the detector; those in (2) that arrive from zenith angles greater than 90 degrees are also degraded in energy by ionization loss in the atmosphere between the rocket altitude and the mirror point. The remainder of the particles, those collected in the upper hemisphere when the rocket is above the atmosphere, comprising more than 80 percent of the particles collected, are at the original energy.

The shape of the trial spectrum after passing through various amounts of atmosphere was constructed from range energy tables (Reference 12). In *principle*, the total contribution to the particle density for the trial function can be calculated by integrating the appropriate energy spectrum at a given point and angle over the entire solid angle of acceptance and collecting area for the known payload orientation at each point on the trajectory, and then integrating over the entire flight. In *practice*, these integrals were approximated by summations. To this sum was added a small contribution for penetration, that is, those particles that crossed the scan line from below, having first traversed the emulsion stack. The absorption length and shift in the energy spectrum resulting from interactions of protons in emulsion are not known well. It was assumed here that an interaction of a proton produced one proton of approximately the same energy and direction; and the contribution from penetration was determined by constructing the shape of the trial spectrum at an absorber depth equal to the amount of atmosphere and emulsion traversed. As seen in Table 1, the contribution resulting from penetration varied from 2 to 23 percent of the sample. The *systematic* error resulting from this procedure was included in the systematic error resulting from the trajectory correction. It should be noted that the contribution from penetration is small and that it is largest at high energies, where the *statistical* error rather than the systematic error governs the total error.

The particle density, in units of particles per cm^2-ster obtained from the procedure outlined above, was then compared with the observed particle density. On the basis of this comparison, a better estimate of the primary spectrum was made, and the procedure was repeated until the trial spectrum produced the observed particle densities. In both flights the second trial spectrum fitted the observed data.

Table 1 shows the contribution to the observed integral intensity that was obtained under various absorber thicknesses for the flight at 1840 UT on 12 November and is typical of all of the rocket flights. The energy E in the table is the energy calculated with the assumption that no absorber was above the emulsion except the wrapping and rocket skin. The table indicates that from 62 to 88 percent of the sample, depending on energy, was obtained at zero atmosphere. The error arising from this procedure is estimated to be essentially zero for that portion of the particles collected above the atmosphere and no more than 30 percent for that portion of the sample collected under some residual

Table 1

Fractional Contribution to Observed Integral Proton Intensity from Various Absorber Depths.

Energy E (Mev)	Fractional Contribution to Proton Intensity Atmosphere (gm/cm^2)							Penetration
	0-0.2	0.2-0.7	0.7-1.5	1.5-6	6-15	15-25	25-35	
15	0.88	0.04	0.03	0.02	0.01	0	0	0.02
20.5	0.86	0.05	0.03	0.02	0.01	0	0	0.03
31	0.82	0.05	0.04	0.03	0.01	0	0	0.05
56	0.76	0.05	0.04	0.04	0.02	0.01	0	0.08
81	0.75	0.05	0.04	0.04	0.02	0.01	0	0.09
120	0.70	0.05	0.05	0.04	0.02	0.01	0	0.13
160	0.66	0.05	0.05	0.05	0.02	0.01	0	0.16
220	0.62	0.05	0.04	0.04	0.03	0.01	0	0.21
270	0.62	0.04	0.04	0.03	0.03	0.01	0	0.23

atmosphere. The estimated error from this source then depends on energy and is of the order of 6 percent for the lower energies ($\leq$81 Mev). The combined error introduced by the uncertainty in measurements of the solid angle of acceptance and the collecting area is 5 percent. Combining this error with the other uncertainties mentioned above gives a root-mean-square (rms) error of about 8 percent at low energies and a somewhat larger value of 10 to 15 percent at high energies (120 to 270 Mev). This systematic error was combined with the statistical uncertainty to yield the errors listed later in the report (Table 3).

Helium Component

To obtain the flux and energy spectra of the helium nuclei in the solar particles, the emulsions flown in the first flight were scanned along a line at a distance 5 mm from the edge of the emulsion. All particle tracks crossing this scan line in the middle half of the emulsion thickness were recorded if they had nine times minimum ionization, or greater, and were within a solid angle defined by $|\beta| \leq 3.5$ degrees and $|\alpha| \leq 45$ degrees. With these criteria, the ambient energy interval was 37.5 to 180 Mev/nucleon. The particle tracks were followed through the emulsion stack until they came to rest or interacted. Grain density and *delta ray** density measurements as a function of residual range were made on about 1200 tracks to resolve helium nuclei from protons. The helium tracks, of which there were 50, were followed from the scan to the outer edge of the emulsion, and those originating from interactions in the emulsion above the scan line were rejected. The very small correction for loss of helium nuclei due to interactions in the emulsion and the shielding was made with

*A *delta ray* is a secondary electron track, originating from the primary track.

an assumed interaction length of 20 cm in emulsion. The ambient energy of the particles was obtained from range measurements except for one particle that interacted in the emulsion. Its energy was determined from a multiple scattering measurement. The scanning efficiency for the detection of helium nuclei was found to be essentially 100 percent.

A similar procedure was followed for obtaining helium nuclei in the second flight. In this case the scan line was 3 mm from the edge, and all particles having an ionization of ≤ 11.0 times minimum, $|\beta| \leq 5.5$ degrees, and $|\alpha| \leq 45$ degrees were recorded. From 1350 particle tracks, 70 helium nuclei having ambient energies between 29 and 130 Mev/nucleon were obtained.

To calculate the flux and energy spectra of the helium nuclei in free space, the effective time and the solid angle are calculated in a manner similar to that for the protons.

Deuterons and Tritons

In the course of analyzing the solar helium nuclei in the first flight, an arbitrary sample of 300 tracks was examined for the presence of deuterons and tritons. The particle tracks scanned and selected for measurements belonged to the following ambient energy intervals: protons, 40 to 56 Mev; deuterons, 50 to 95 Mev; and tritons, 60 to 130 Mev. Integral delta ray counts were made over the last 2 mm of range. From a plot of the frequency distribution of delta rays, about 100 tracks were selected that would contain 80 percent of the deuterons and tritons present in the entire sample of 300 tracks. Accurate ionization and range measurements were made on these tracks to resolve protons, deuterons, and tritons.

Heavy Nuclei

To determine the heavy nuclei characteristics in the solar cosmic ray event, a complete scan of the periphery of the nuclear emulsion disks, 0.7 mm from the edge, was made for tracks of heavy nuclei within a solid angle, $|\beta| \leq 20$ degrees and $|\alpha| \leq 45$ degrees. The scanning efficiency safeguards and checks, including additional scanning farther in from the edge of the plates than the original scan (at 2.5 and 6.5 mm from the edge), were similar to those used for the proton component. There was no indication of particles being missed.

After elimination of the tracks that could be identified as having been formed by helium nuclei, measurements were made on the remainder to determine the charge and energy of the primary nucleus that produced each track. For this purpose, it was sufficient to record the range of the particle and its relative rate of energy loss. The very small number of heavy tracks having energies sufficiently high that they did not come to rest in the stack was found to be consistent with that expected from the normal high energy galactic cosmic ray flux. Therefore the range could be used as one parameter for the solar heavy nuclei. The range of a heavy nucleus is given by the expression (Reference 13):

$$R_H = \left(\frac{M}{Z^2}\right) R_{proton} + R_{ext} \quad , \tag{1}$$

where R_{ext} is a very small term. Since R_{proton} is a function of v/c and known constants, and R_{ext} is known, Equation 1 gives R_H in terms of Z and v/c.

To determine the relative rate of energy loss, the delta ray density method was used, since it gave a more reliable estimate of the charge than the thin-down or effective track width measurements. Both the four-grain delta ray density criteria and the method of counting delta rays whose projected length in the emulsion plane extended beyond two parallel lines at a fixed distance on each side of the primary track were tried. The resolution obtained by the two methods was similar, with the latter being slightly better. To provide an adequate length for charge resolution measurements, a range of at least 1 mm in the emulsions was demanded for all tracks included in the final analysis. This restriction, plus the material between the emulsion and the ambient radiation, set the lower limit on the energy.

Since the delta ray density varies with the degree of development, the matter of variations in development must be considered. In general it seemed better to try to avoid variations rather than to correct for them, and this was done whenever possible. Therefore the delta ray density over a given length was measured rather than the integral number of delta rays from the end of the track; in this way most of the nonuniformities now to be discussed could be avoided with relatively little loss in resolution because of slightly reduced statistics. Since a large number of acceptable heavy nuclei tracks was found in each plate (about fifty in the first flight and eighty in the second), a self-consistent charge calibration was possible for each plate; thus the problem of emulsion-to-emulsion development variations was circumvented. For a small portion of the tracks, a count was necessary in *two* plates to obtain the desired statistics; in these cases a statistically weighted average of the Z determination was used as the final value. The emulsion-to-emulsion variations in delta ray density were $\lesssim$ 3 percent in these plates.

There are also several kinds of sensitivity variations that can occur within an emulsion plate. Nonuniformity with depth can usually be largely avoided by use of known developing procedures. The variation of grain density with depth for a plate from the first flight is shown in Figure 3, for example. In addition, delta ray measurements were not made in the top or bottom 15 μ in any case and were made in the top or bottom 45 μ for only approximately 10 percent of the tracks, where a meaningful measurement could not be made on the track without so doing. The counting was performed at the same distance in from the edge whenever possible, and the small correction for average development over the length of the count was made for the few cases where this was not possible. Figure 4 shows the variation of grain density with distances in from the plate edge. The plates were further

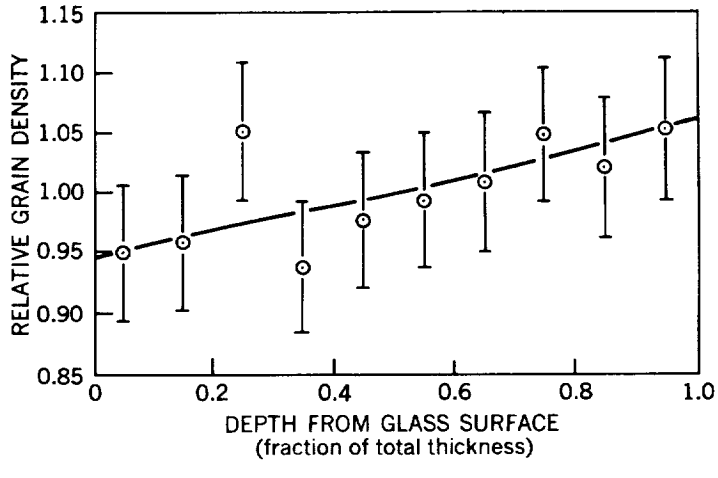

Figure 3—The variation of grain density with depth in emulsion as obtained from measurements on tracks of fast particles.

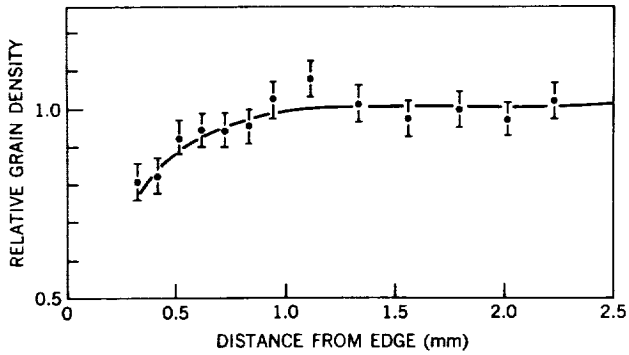

Figure 4—The variation of grain density as a function of the distance from the emulsion edge as obtained from tracks of fast particles.

examined for local nonuniformities. For the relation between delta ray varations with grain density variations, it was necessary to use high energy heavy tracks of the appropriate delta ray density in cosmic ray plates developed to a similar degree and with similar grain size, since no tracks of this type were found in the short solar particle exposure. However, since the correlation should be nearly the same and since the correction for sensitivity gradients was usually small compared with the statistical uncertainty — 2 to 3 percent on the average compared with 6 to 10 percent — no significant error should be introduced by this procedure.

The general subject of delta ray counting, associated uncertainties, and statistical errors is complex; however, it has already been treated extensively (References 10, 14, and 15), and therefore only a few more remarks will be added. For observer consistency, it is advisable to recount standard tracks of various delta ray densities frequently—and this was done herein. The constant correction for background electrons is very small compared with the delta ray densities measured in the region of interest: approximately 1 percent of the plateau value for oxygen.

The variation of the delta ray density with v/c as measured by the second delta ray density method (namely, counting those secondary electrons whose projected length in the emulsion plane extends beyond some fixed distance) was found to agree well with Mott's formula, which was shown previously to be a good representation of the experimentally observed distribution (References 14 and 15). The correction for the difference between the average of the delta ray density measured over a finite length and the theoretical value at the midpoint was made with this formula. Again, the correction is small compared with the statistical uncertainty. There is no simple model giving the variation of the four-grain delta ray density with range because the variation in track width with range causes the cutoff energy corresponding to a delta ray with four observable grains to change. Experimental curves can be developed, and were obtained. However, as mentioned earlier, the former method gave better resolution; and those results are presented as Figure 5.

By a method described in detail in a previous paper (Reference 10), the charge resolution obtained experimentally for the medium nuclei was found to be 0.27 of a charge. This is about the same as the average rms uncertainty for charge determination in this charge group, as expected from statistical uncertainty. For nuclei with charges of 10 or more, the accuracy begins to decrease slowly with charge. A correction was made to the nitrogen abundance for the effect of adding particles from the tails of the carbon and oxygen components (Reference 10). However, since the correction is significant, it is perhaps best to regard the nitrogen abundance as an approximate upper limit. The limits set for the fluorine and boron components are due primarily to the oxygen and carbon tails respectively. A diagram showing the charge resolution for tracks from the first flight is shown in Figure 6; the resolution for the other flight was similar. In addition to the experimental points, the

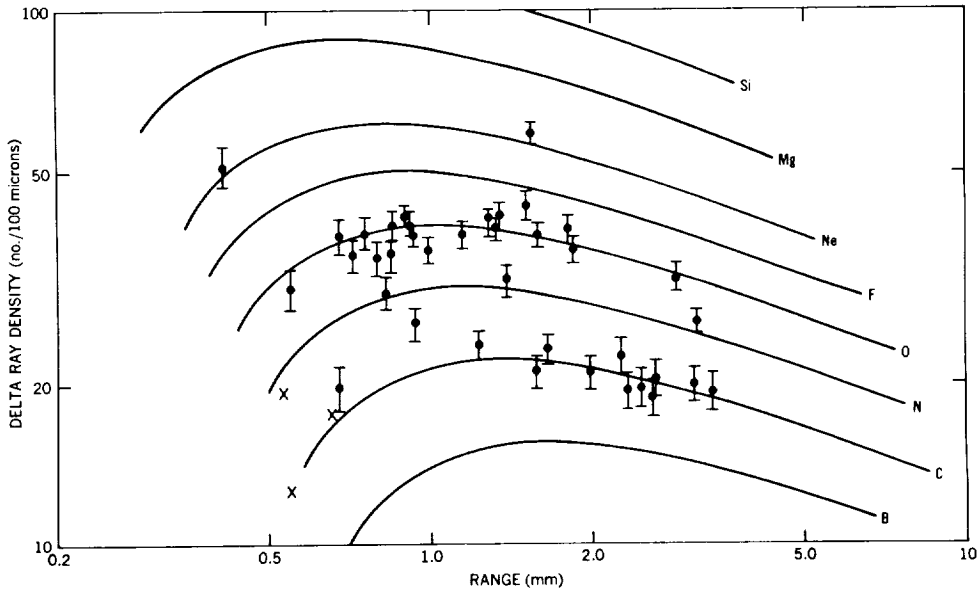

Figure 5—Plot of delta ray density as a function of range for measurements made within a single plate. A few tracks for which N_δ exceeded $100/100\mu$ are not shown, as well as one for which the range exceeded 10 mm. The length of the vertical line associated with each point gives the uncertainty due to the number of delta rays only counted. The small corrections for development variation have been made for the cases where it was not negligible, as explained in the text. Points marked with a cross were not included in the final results because, although they satisfied the range criteria, they correspond to particles whose energies were below the cutoff limit.

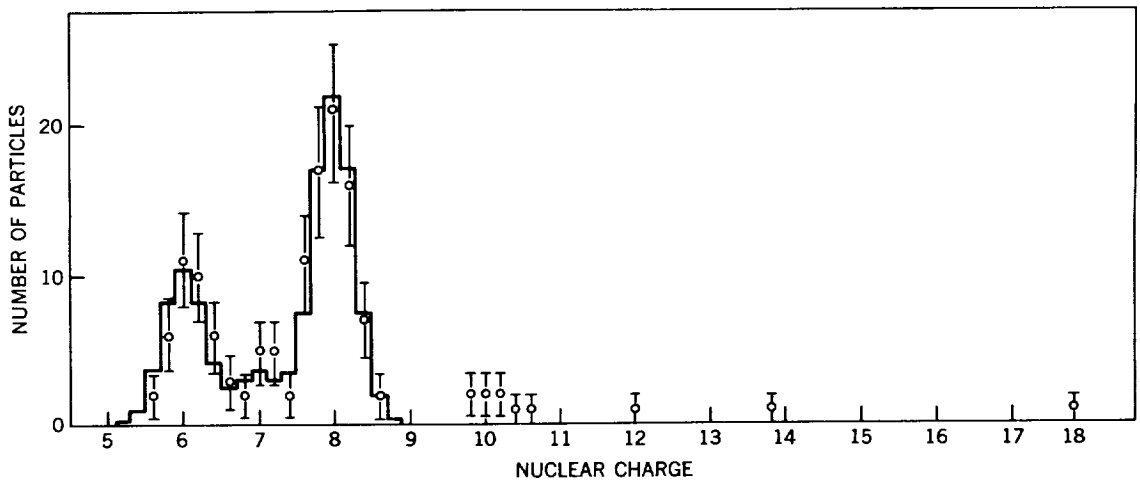

Figure 6—The charge distribution for heavy nuclei from the flight at 1840 UT on November 12. The experimental points are marked by open circles. The expected distribution for an rms uncertainty of 0.27 of one charge for medium group of nuclei is shown by the solid histogram, assuming the relative abundances of B, C, N, O, and F nuclei to be 0, 5, 1.7, 10, and 0, respectively.

expected distribution for an rms uncertainty of 0.27 charge is shown, assuming the relative abundances of B, C, N, O, and F to be 0, 5, 1.7, 10, and 0 respectively.

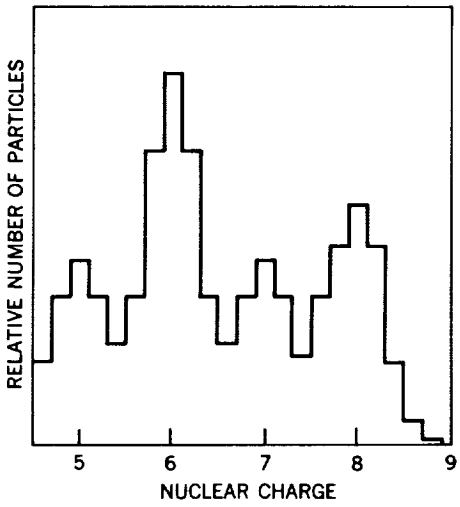

Figure 7—The calculated charge distribution for a composition similar to that of galactic cosmic radiation, assuming the same charge resolution as shown in Figure 6. The relative abundances of B, C, N, O, and F nuclei were assumed to be 1, 2, 1, 1.3, and 0 respectively.

For comparison, Figure 7 gives the expected histogram for a composition similar to that of galactic cosmic radiation for the same charge resolution. For this histogram the relative abundances of B, C, N, O, and F were taken to be 1, 2, 1, 1.3, and 0 respectively. The number of particles obtained for each interval in such a diagram is usually of the order of five. Thus, except for carbon, the distribution shows less pronounced peaks than is the case for the solar particles—especially if there are a few large fluctuations. A typical distribution of this type is shown in Reference 14, in which the expected error is similar to the present experiment because of the fact that, though the statistical error is somewhat less by a factor of about 0.75, the problem of plate-to-plate normalization necessitated by the low galactic heavy flux approximately compensates for this effect. The degree of resolution in the present experiment may also be helped somewhat by the particularly favorable development of this set of plates.

The resolution would be expected, then, to be similar to ordinary cosmic ray studies–as it is–and what appears to be a sharper resolution, on first glance at Figure 6, is in reality only a reflection of the different composition of the two radiation types.

The only subject related to the charge measurements still to be discussed is the matter of absolute charge calibration. The particular difficulty was the complete absence of low energy light nuclei (Li, Be, and B), which meant that there was a gap of several charges between helium nuclei and the higher charges. The expected normalizing constant for the curve of the delta ray density N_δ as a function of range R was obtained in two ways: first, from the tracks of carbon and oxygen nuclei in normal cosmic ray balloon flight nuclear emulsion plates developed to the same degree and, second—and with less certainty—from the helium nuclei curve in these plates. Whereas the latter method was used only as a check, the former method should lead to an error of no more than 0.2 charge. In fact the experimental points predominately clustered so well around the expected curves for carbon and oxygen that the final best curves, based on assuming the tracks to be formed by these nuclei, differed from the expected curves by less than 0.1 charge.

To calculate the flux and energy spectra of the heavy nuclei in free space, a procedure essentially identical to that for the proton component was used. As shown in Table 2, the contribution during the ascent and descent phase is smaller than for the protons, because of the steeper energy spectrum and the higher rate of energy loss per nucleon. Again, because of the wall and the minimum track length accepted for analysis, there was always about 0.61 gm/cm^2 of material in the payload for any acceptable particle to go through. Therefore, the cutoff energy remained essentially constant for most of the

Table 2

Fractional Contribution to Observed Integral Medium Nuclei Intensity from Various Absorber Depths.

Kinetic Energy per Nucleon (Mev)	Fractional Contribution to Medium Nuclei Intensity				
	Atmosphere (gm/cm^2)				
	0-0.2	0.2-0.7	0.7-1.5	1.5-6	6
42.5	0.96	0.03	0.01	≈ 0.002	0
54.9	0.95	0.03	0.02	≈ 0.003	0
68.8	0.94	0.03	0.02	≈ 0.005	0
95	0.92	0.04	0.03	0.01	≈ 0.005

effective collecting time and solid angle. For a similar reason, the effective collection times for the heaviest nuclei accepted were nearly the same as those of the medium nuclei, although the minimum energy per nucleon (determined by the minimum accepted range) increased with charge.

RESULTS

Singly Charged Particles

From the measurements described in the section "Proton Component," the integral and differential energy spectra of solar protons in the kinetic energy interval from 14.5 to a few hundred Mev were obtained. The flux values measured in the two rocket flights are given in Table 3. The integral flux above 340 Mev in the first flight and 270 Mev in the second was estimated by extrapolating the differential energy spectra. These values are such that the uncertainty introduced into the integral flux values is negligible except for the highest energy points quoted.

The errors shown in the integral flux values included both the statistical and systematic errors that enter into the measurements. In the integral flux values the statistical errors are 6 percent in the energy interval from 14 to 81 Mev and then gradually increase from 6 to 25 percent in the energy interval from 120 to 340 Mev. Systematic uncertainty is given in the section "Proton Component." The differential flux was calculated from the integral flux values. The error was obtained by calculating the statistical error as that arising from the statistical errors of the two integral points and combining this error with the systematic uncertainty to obtain the total error.

The differential energy spectra of solar protons in the two rocket flights shown in Figure 8 indicate that very significant changes occurred. In the second flight the intensity of low energy protons had increased, while that of high energy protons had decreased as compared with those in the first flight.

The proton spectrum cannot, at any time of measurement, be represented by a power law spectrum of the form

$$\frac{dN}{dE} = KE^{-n} , \qquad (2)$$

Table 3

Integral and Differential Flux Values for Protons.

Kinetic Energy (Mev)	Flux at 1840 UT Nov. 12, 1960	Flux at 1603 UT Nov. 13, 1960
Integral Flux (particles/cm²-ster-sec)		
15	1690 ± 190	5160 ± 520
20.5	1290 ± 140	3690 ± 370
31.3	850 ± 94	2180 ± 240
56	501 ± 55	842 ± 81
81	310 ± 34	350 ± 39
120	127 ± 15	78 ± 9
160	69 ± 10.4	27 ± 4
220	24.3 ± 5.4	6.6 ± 1.3
270	8 ± 3.0	
Differential Flux (particles/cm²-ster-sec-Mev)		
17.5	73 ± 24	267 ± 72
25.5	40.7 ± 12	140 ± 26
43	14.1 ± 3.5	54 ± 8
68	7.6 ± 1.9	19.7 ± 3.1
100	4.7 ± 1.1	7.0 ± 0.9
138	1.45 ± 0.35	1.3 ± 0.2
186	0.74 ± 0.18	0.34 ± 0.06
243	0.33 ± 0.12	0.08 ± 0.03
306	0.10 ± 0.04	

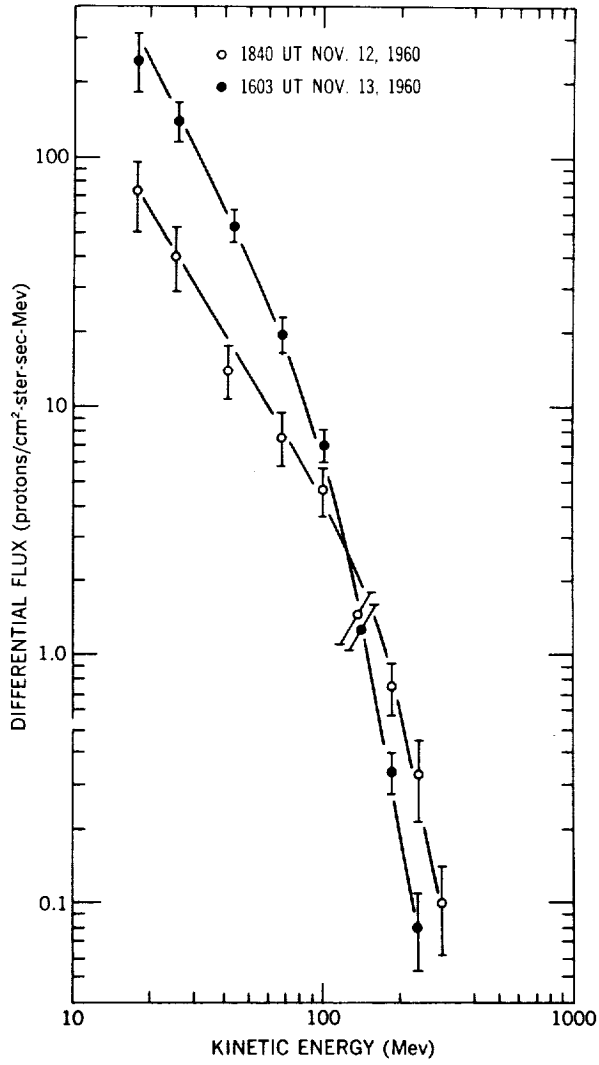

Figure 8–Differential kinetic energy spectra of protons during the two flights.

where E is the proton kinetic energy, in Mev, and K and n are constants. Consider, for example, the first flight, where

$$\frac{d\ \ln\left(\frac{dN}{dE}\right)}{d\,(\ln E)}$$

varies from about 1.5 in the energy interval from 15 to 40 Mev to a value of about 5 in the energy interval from 200 to 300 Mev. In the second flight, the spectrum behaves in a similar manner. This feature was even more pronounced in the results obtained during the September 3, 1960, flare event (Reference 16).

An alternative way of expressing the proton energy spectrum is as a power law of the total energy:

$$\frac{dN}{dE} \quad \frac{C}{\left(1 + \frac{E}{W_0}\right)^{\gamma}} \quad \frac{C}{\left(\frac{W}{W_0}\right)^{\gamma}} , \tag{3}$$

where W is the total energy and W_0 is the proton rest energy. The data from the two flights are plotted in this form in Figure 9. A proton spectrum of this form fits the experimental data well in the energy interval from 35 to 300 Mev, with γ about 21 in the first flight and γ about 37 in the second. In the event of September 3, 1960, this form also fits the data well in the entire energy interval from 30 to 600 Mev, as measured by rocket (Reference 16) and balloon-borne (Reference 1) detectors. It is not possible to distinguish between a spectrum of the form given by Equation 3 and the form given below by Equation 4 from the data of this work since, for $E/W_0 \ll 1$, Equation 3 reduces to this form:

$$\ln \frac{dN}{dE} \quad \ln C - \frac{E}{E_0} , \tag{4}$$

where $E_0 = W_0/\gamma$.

Another feature of the proton energy spectrum is that, at about 35 Mev, the slope abruptly changes to a large value, as shown in Figure 9; this is present in both flights. The data of September 3, 1960, show a similar, but less marked, change in slope. This abrupt change occurs at nearly the same energy in each case, although the slopes of the energy spectra above 35 Mev are very different.

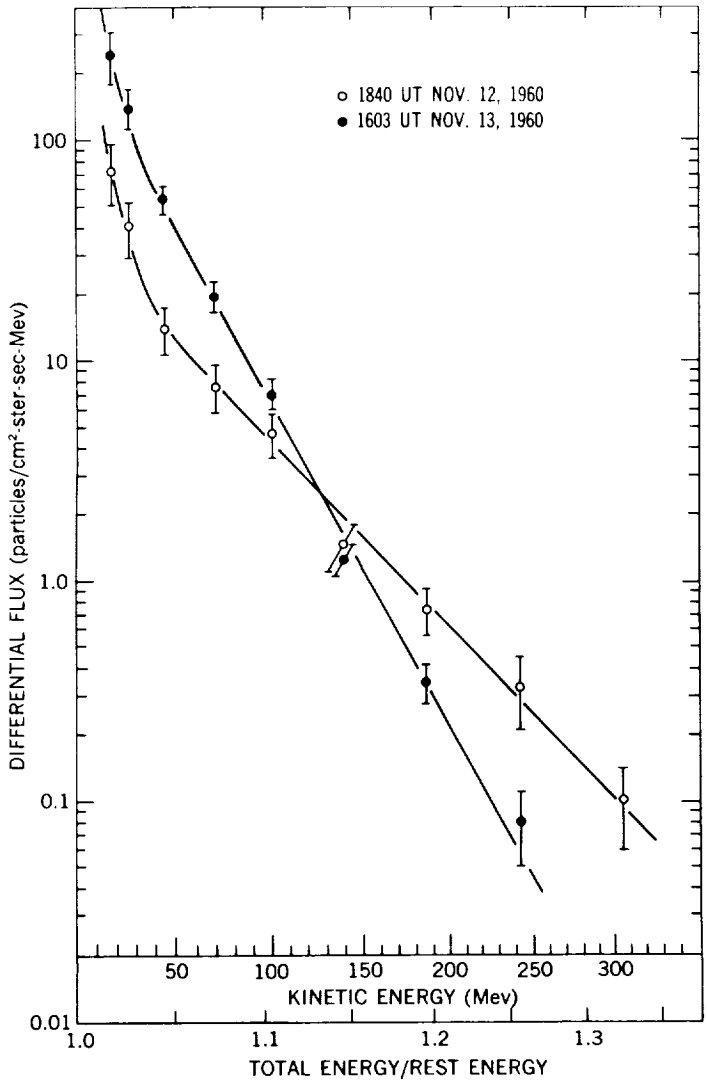

Figure 9—Differential proton flux as a function of total energy units of the rest energy. Note that the abscissa is an expanded logarithmic scale.

As mentioned in the section "Deuterons and Tritons," a set of 300 solar cosmic ray particles was examined for the presence of isotopes of hydrogen other than protons. After elimination of 15 helium particles, there remained 284 protons, one deuteron, and no tritons. A small number of secondary

deuterons and tritons is produced in interactions of other particles in the air and is recorded in the emulsion while on the ground, and during the ascent and descent of the detector through the atmosphere. In the area and solid angle scanned, the probability of finding a deuteron or triton from these sources is a few tenths. Therefore the flux of deuterons and tritons in the solar particles is less than 1 percent of the protons in comparable energy intervals and, in the present experiment, there is no positive evidence for any.

Helium Nuclei

The differential energy spectra of solar helium nuclei measured in the two flights are shown in Figures 10 and 11 and in Table 4. In the first flight the flux of solar particles in the energy range

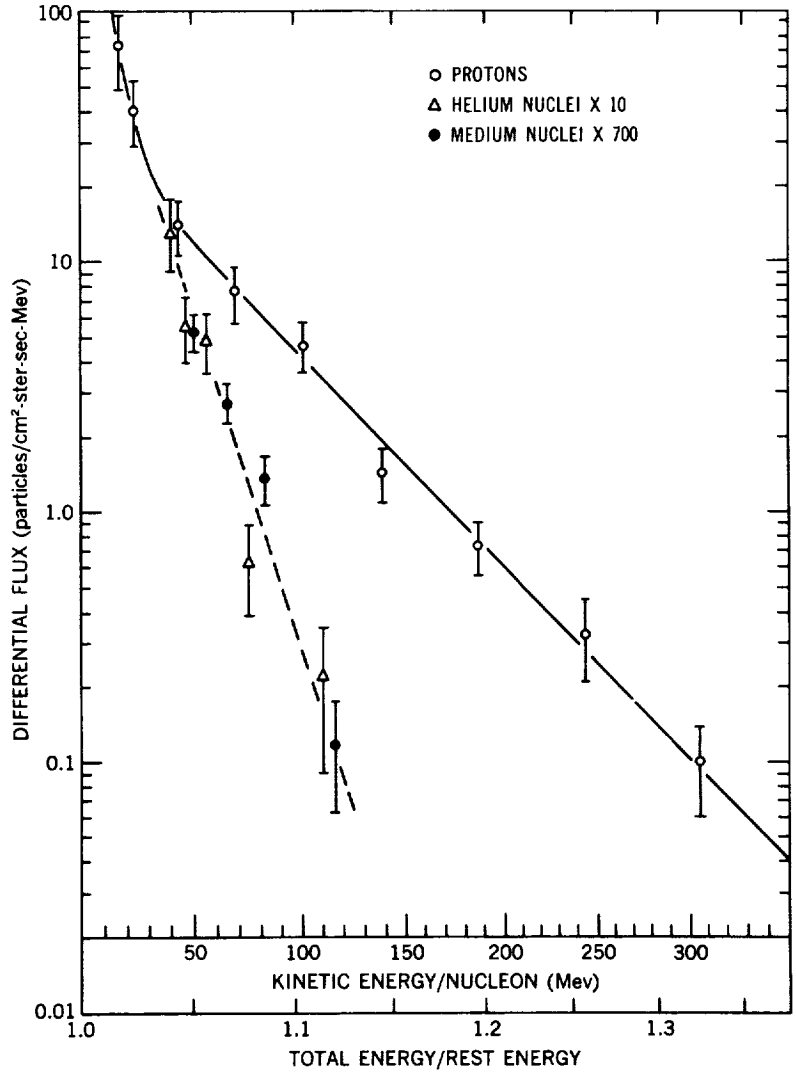

Figure 10—Differential spectra for protons, helium nuclei, and medium nuclei as a function of the total energy per nucleon in units of nucleon rest energy at 1840 UT November 12, 1960. Note that the abscissa is an expanded logarithmic scale.

from 37.5 to 130 Mev/nucleon was 18.3 ± 2.8 particles / cm^2 - ster - sec. In the second flight on November 13, a still higher flux of 41.4 ± 6.2 particles/cm^2-ster-sec was seen in the same energy interval. Figures 10 and 11 indicate that the spectra can be expressed in the form of Equation 3. The value of γ was 63 ± 7 in the first flight and 68 ± 7 in the second flight.

Ney and Stein (Reference 2) measured solar helium nuclei from this flare in balloon flights from Minneapolis at about 1900 UT on November 13. Because this balloon flight was only about 3 hours after the second rocket flight and the helium flux presumably did not change appreciably, we may compare the two results. Their differential helium flux of 0.02 ± 0.003 and 0.009 ± 0.0015 particles/cm^2-ster-sec-Mev at 100 and 112 Mev / nucleon respectively agrees well with the results in Figure 11.

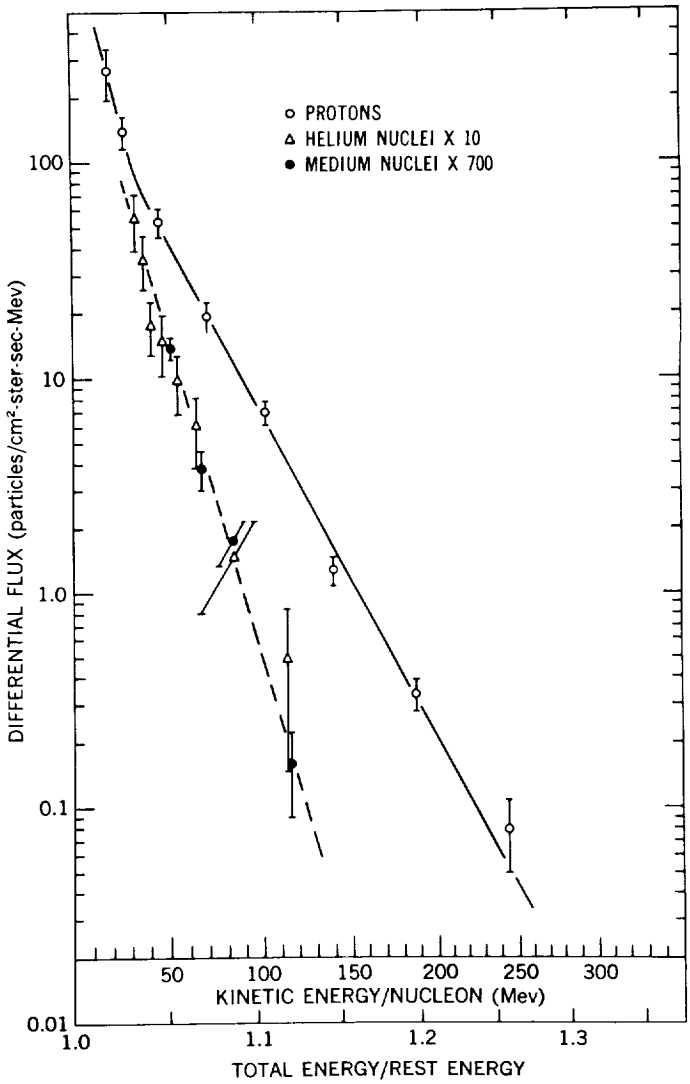

Figure 11—Differential spectra for protons, helium nuclei, and medium nuclei as a function of the total energy per nucleon in units of nucleon rest energy at 1603 UT November 13, 1960. Note that the abscissa is an expanded logarithmic scale.

Heavy Nuclei

With the flux and energy/nucleon spectra of the heavy nuclei obtained, a large low energy component — energy / nucleon < 300 Mev — was found in each of the flights, as was a high energy component—energy/nucleon > 300 Mev—that was consistent with the normal cosmic ray background. It has been shown previously (Reference 3) that the normal cosmic ray flux of low energy heavy nuclei is no more than a few particles/m^2-ster-sec and can therefore be neglected. Hence this large low energy component represents the accelerated solar heavy nuclei.

The heavy particles that were included in the analysis—that is, those whose emulsion equivalent range was greater than 1.7mm—were found to be predominantly medium nuclei ($6 \leq Z \leq 9$), rather than light nuclei ($3 \leq Z \leq 5$) or *large nuclei** ($Z \geq 10$). Therefore the discussion of the heavy nuclei will begin with a treatment of the properties of the medium nuclei since, in addition to being the most abundant heavy nuclei, they also have nearly the same charge and the same charge-to-mass ratio.†

*The term *large nuclei* is introduced here to avoid the confusion that has arisen in the cosmic ray and astronomical literature resulting from *heavy* being used to refer both to nuclei with charges greater than 2 and to those with charges greater than 9.

†Fluorine, of course, does have a slightly different ratio from the others, namely 9:19 instead of 1:2 for the predominant isotope of each of the other three, but there is no positive evidence for fluorine among the solar particles and it is relatively rare in general.

Table 4

Differential Flux of Helium Nuclei.

Kinetic Energy Interval (Mev/nucleon)	Flux in the Interval $\left(\frac{\text{particles}}{\text{cm}^2\text{-ster-sec}}\right)$	Differential Flux $\left(\frac{\text{particles}}{\text{cm}^2\text{-ster-sec-Mev}}\right)$
At 1840 UT November 12, 1960		
37.7 - 42.5	6.45	1.34 ± 0.42
42.5 - 50	4.18	0.56 ± 0.16
50 - 60	4.85	0.49 ± 0.13
60 - 90	1.92	0.064 ± 0.026
90 - 130	0.89	0.022 ± 0.013
At 1603 UT November 13, 1960		
29.0 - 32.5	19.53	5.58 ± 1.68
32.5 - 35.5	10.98	3.66 ± 1.06
35.5 - 41.5	10.80	1.80 ± 0.52
41.5 - 47.5	9.06	1.51 ± 0.48
47.5 - 57.5	9.90	0.99 ± 0.30
57.5 - 67.5	6.10	0.61 ± 0.23
67.5 - 95	4.24	0.15 ± 0.07
95 - 130	1.77	0.05 ± 0.035

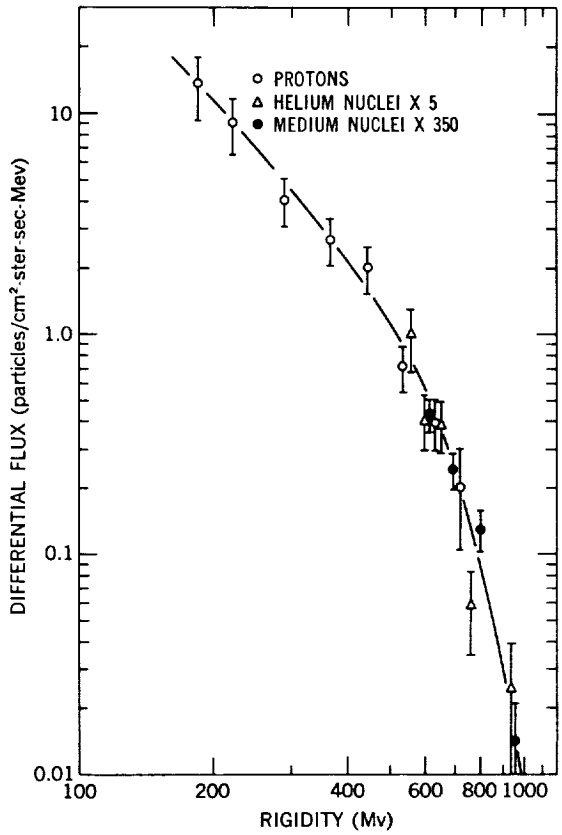

Figure 12—Differential spectra of protons, helium nuclei, and medium nuclei as a function of rigidity at 1840 UT November 12, 1960.

The differential energy per nucleon and rigidity spectra for medium nuclei are plotted in Figures 10 and 12 for the flight at 1840 UT November 12, and in Figures 11 and 13 for the flight at 1603 UT November 13, and are given in Table 5. An extrapolation of the energy spectra to balloon altitudes would indicate that solar heavy nuclei even in this very large event are barely detectable at that level. This result explains why heavy nuclei have in general not been seen at balloon altitudes during solar cosmic ray events in the past.

The other subject of interest in the study of the heavy nuclei is the charge spectrum, which is given in Table 6. Notice that within the medium group oxygen is somewhat more abundant than carbon, as spectroscopic evidence of the sun (References 17 and 18) indicates—contrary to the situation in normal cosmic rays. The fact that nitrogen is appreciably less abundant than carbon or oxygen is also in agreement with spectroscopic measurements of the sun.

The lack of any positive evidence for light nuclei and the relatively low limit set for their abundance is consistent with the relative abundance of this group in the sun (where they are less abundant than medium nuclei by a factor of 10^{-6} or more) and with the very small amount of material the solar

heavy nuclei have gone through. The ratio of light nuclei to medium nuclei in galactic cosmic rays at the top of the atmosphere is approximately 0.3 and is usually assumed to be essentially zero at the source.

There are small but measurable fluxes of the large nuclei; however the abundance comparison to other species must be made at higher energies because the range of a nucleus for a given energy per nucleon, or velocity, is a decreasing function of the quantity Z^2/M. Neon is

Table 5

Differential Flux of Medium Nuclei

Kinetic Energy Interval (Mev/nucleon)	Flux in the Interval $\left(\frac{\text{particles}}{\text{m}^2\text{-ster-sec}}\right)$	Differential Flux $\left(\frac{\text{particles}}{\text{m}^2\text{-ster-sec-Mev}}\right)$
At 1840 UT November 12, 1960		
42.5 - 54.9	969	78 +13
54.9 - 68.8	548	39.4 ± 7.4
68.8 - 95	521	19.9 ± 4.5
95 - 135	68	1.7 ± 0.8
At 1603 UT November 13, 1960		
42.5-54.9	2463	198± 24
54.9 - 68.8	762	55 ±12
68.8 - 95	663	25 + 6
95 - 135	91	2.3 ± 1.0

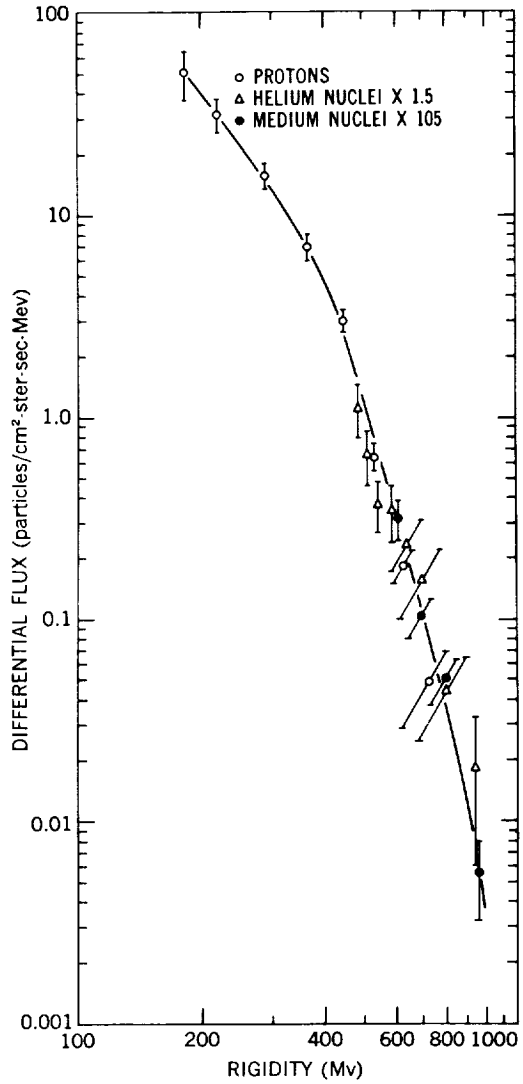

Figure 13–Differential spectra of protons, helium nuclei, and medium nuclei as a function of rigidity at 1603 UT November 13, 1960.

Table 6

Charge Spectrum of Heavy Nuclei in the Same Velocity Interval with a Base of 10 for Oxygen

Time	Nuclear Charge						
	$_4$Be - $_5$B*	$_6$C	$_7$N	$_8$O	$_9$F	$_{10}$N	$_{11}$Na - $_{18}$A
1840 UT Nov. 12, 1960	< 0.2	4.8 ±1.0	1.7 ±0.7	10	< 0.3	1.4 ± 0.5	1.1 ± 0.7
1603 UT Nov. 13, 1960	< 0.2	7.1 ±1.5	1.9 ±0.8	10	< 0.3	1.2 ± 0.5	1.6 ± 0.7
Average:	< 0.2	6.0 ± 0.9	1.8 ± 0.5	10	< 0.3	1.3 ± 0.4	1.4 ± 0.5

*Lithium ($Z = 3$) is not included because the scanning efficiency for Li tracks was less than 100 percent. Whenever Li occurs in nature, however, its abundance is similar to that of Be and B.

seen from Table 6 to be 0.13 ± 0.04 of the abundance of oxygen. There is no spectral evidence to indicate what the abundance of neon in the sun is; however, on the basis of stellar models, there is no reason to expect the abundance of neon relative to medium nuclei to be very different from the cosmic abundances (Reference 19), where the neon to oxygen ratio is a few tenths. Table 6 indicates that nuclei with a charge greater than 10 were quite rare. The ratio of nuclei with charges $11 \leq Z \leq 18$ to oxygen nuclei in the same velocity interval is found to be 0.14 ± .05 compared with the order of 0.09 given by spectroscopic evidence of the sun. The ratio of nuclei with $11 \leq Z \leq 18$ to medium nuclei in the solar cosmic rays of November is 0.08 ± .03 compared with 0.25 ± 0.08 for galactic cosmic rays at the top of the atmosphere and 0.35 ± 0.10 for galactic cosmic rays extrapolated back to their source (Reference 20).

There was one very large nucleus of low energy, probably in the iron group; but, since this could have been a cosmic ray particle, no definite statement about detection of solar nuclei in this charge group can be made. If the nuclei in this group of very large charges occur in the same relatively small abundance as in the sun, their presence would not have been detected in the samples reported here.

Comparison of Hydrogen, Helium, and Medium Nuclei

Since the flux and the energy spectra of solar protons, helium nuclei, and medium nuclei have been obtained, a comparison of these three components can be made. The differential energy spectra are plotted in Figure 10 for the first flight and in Figure 11 for the second flight. The energy spectra of the helium and medium nuclei have the same slope within uncertainties in both flights. On the other hand, the slope of the energy spectrum of the helium nuclei, or the medium nuclei, is much steeper than that of the proton component. Specifically γ, defined by Equation 3, was 21 ± 2 for the proton component and 63 ± 7 for the multiply charged particles in the first flight; and the corresponding numbers for the second flight were 37 ± 2 and 68 ± 7.

The differential rigidity spectra of these three components are plotted in Figures 12 and 13 for both flights. These figures show that the rigidity spectra of hydrogen, helium, and medium nuclei are similar; however the proton data at the high rigidity end of the spectrum are of poor statistical weight and only extend up to about 800 Mv as compared with 1000 Mv for the multiply charged particles.

In Table 7, the relative abundances of protons, helium, and medium nuclei are listed for equal energy per nucleon intervals and equal rigidity intervals for the two flights. For comparison, the values obtained in the September 3, 1960, event (Reference 3) and the preliminary results for one firing (Nov. 16) in the November 15, 1960, event* are also given. The relative abundances for the same energy per charge are intermediate between those for the same energy per nucleon and the same rigidity. The lower limit of 42.5 Mev/nucleon in Table 7 was set by the material above the emulsion and the minimum length of track required to identify the medium nuclei. The upper limit of 95

*Biswas, S., Fichtel, C. E., and Guss, D. E., "Rocket Observations of Solar Protons, Alpha Particles, and Heavy Nulcei from November 15, 1960, Flare." Paper presented at 43rd Annual Meeting, American Geophysical Union, Washington, April 1962. Abstract published; entire paper will be published in *Proceedings*.

Table 7

Relative Abundances of Protons, Helium Nuclei, and Medium Nuclei.

Time	Proton / Medium Nuclei	Proton / Helium Nuclei	Helium Nuclei / Medium Nuclei
42.5 Mev ≤ Kinetic Energy/Nucleon ≤ 95 Mev			
1840 UT Nov. 12, 1960	2000 ±400	32 ± 6	63 ±14
1603 UT Nov. 13, 1960	2650 ±430	36 ± 7	72 ±16
Average:	2330 ±290	34 ± 5	68 ±11
1408 UT Sept. 3, 1960	2650± 790	32 ± 10*	83 ±32*
1951 UT Nov. 16, 1960	1870± 360*	26 ± 7*	77 ±20*
570 Mv ≤ Rigidity ≤ 870 Mv			
1840 UT Nov. 12, 1960	300 ± 55	5 ± 1	63 ±14
1603 UT Nov. 13, 1960	68 ± 14	1 ± 0.2	72 ±16
1408 UT Sept. 3, 1960	1100 ±380	13 ± 5*	83 ±32*
1951 UT Nov. 16, 1960	105 ± 35*	1.4 ± 0.3*	77 ±20*

*Preliminary value; final value to be published later.

Mev/nucleon was chosen because essentially all of the multiply charged particles observed had energies less than this value and there were no proton data above the corresponding rigidity value. These limits in rigidity correspond to 570 and 870 Mv respectively for helium and medium nuclei with a charge to mass ratio Z/M of 0.5. The proton energies corresponding to 570 and 870 Mv are 160 and 338 Mev respectively.

Since the helium and medium nuclei have the same energy spectrum, the helium to medium nuclei ratio is *not* a function of energy. The proton to helium nuclei ratio and also the proton to medium nuclei ratio are, however, functions of energy since their energy spectra differ. The proton to helium nuclei ratio as a function of energy is shown in Table 8 for both flights.

Table 7 shows that the proton to helium nuclei and the proton to medium nuclei ratios in the same rigidity interval both vary greatly from one flight to another. On the other hand, the proton to helium nuclei and the proton to medium nuclei ratios in the same energy per nucleon intervals are nearly the same each time. Thus there is the striking situation that, although the energy per nucleon spectra for protons and multiply charged particles are different, the relative abundance of protons with respect to the others remains markedly constant in the energy interval examined.

DISCUSSION

Since the relative abundances of the energetic nuclei reaching the earth in a major solar particle event have been obtained and the energy spectra of the major components determined at two different times in the event, a number of old hypotheses can be reexamined and a few new ideas put forth.

Table 8

Ratio of Differential Flux of Protons to That of Helium Nuclei as a Function of Kinetic Energy Per Nucleon.*

Time	$(dJ_p/dE)/(dJ_{He}/dE)$ Kinetic Energy (Mev/nucleon)				
	40	60	80	100	120
At 1840 UT Nov. 12, 1960	14	32	72	165	350
At 1603 UT Nov. 13, 1960	21	45	78	145	250

*These ratios are obtained from the best fitting lines for the differential spectra of protons and multiply charged nuclei. Since helium and medium nuclei have the same energy spectra, the values for $(dJ_p/dE)/(dJ_m/dE)$ may be obtained by multiplying the above ratios by a factor of about 70. The error for the ratio at the lowest energy is about 30 percent and increases to about 50 percent at the highest energy.

Modulation and Diffusion

In this section the problem of the interplanetary history of the energetic solar particles will be reviewed with emphasis on those areas relating to the results of this work. Since the particles seen at the earth already have been acted on by both the acceleration phase at their source and the transit phase, wherein they are modulated by the interplanetary conditions, it is necessary to try to disentangle the two effects. We will proceed from the observations back to the source, and the discussion will begin with the transit phase.

Parker* has shown that particle diffusion must predominate over particle drift in the interplanetary space because of the associated time scales. Several diffusion models for solar cosmic ray particles have been developed (References 21 and 22, and Parker*), and in general the diffusion coefficient that determines the rate of diffusion depends both on the particle velocity and on its rigidity. Parker suggests that, below a proton energy of the order of 1 Bev (the corresponding rigidity is approximately 2 Bv), the diffusion coefficient depends primarily on the velocity of the particle and not on the rigidity, because in this rigidity interval the radius of particle gyration is less than the scale length of the magnetic field disordering. If this latter proposition is correct, we would expect the ratio of the differential proton energy spectrum† dJ_p/dE to the differential helium energy per nucleon spectrum dJ_{He}/dE at a given energy E per nucleon to be independent of time in the event at energies included in our study.‡ Remember that the medium nuclei energy per nucleon spectrum was the same as that for helium within uncertainties; so in this discussion either the medium nuclei or the helium nuclei could be compared with the proton component.

The two exposures studied here occurred at very different times in the November 12, 1960, event—about 5 hours and 27 hours from the flare's beginning and probably under very different interplanetary

*E. N. Parker, private communication of work to be published.

†Writing the differential spectra as a function of energy per nucleon is, of course, equivalent to writing it as a function of velocity for purposes of comparison, since two nuclei with the same energy per nucleon have the same velocity.

‡This conclusion should not necessarily be made for balloon altitude experiments where the particle rigidities are higher and consequently closer to what is only an order of magnitude limit for the rigidity.

conditions (Reference 4). These exposures therefore provide a good test of this hypothesis concerning the diffusion coefficient. In spite of the facts that the differential energy spectrum is very different from one flight to the next for a given component and that the slope of the helium curve is different from that of the proton one at a given energy per nucleon, the ratio $(dJ_p/dE)/(dJ_{He}/dE)$ is found to be the same within uncertainties for the two flights for those energies where comparisons can be made, as shown in Table 8. On the other hand, the ratio $(dJ_p/dR)/(dJ_{He}/dR)$, where R is the rigidity, is very different. This result and the fact that similar abundances are seen in the same velocity intervals for three events are then in agreement with the prediction that the velocity predominates over the rigidity in the diffusion coefficient in this low rigidity interval—at least in these three events.

The experimental result of the near constancy of the ratio $(dJ_p/dE)/(dJ_{He}/dE)$ from one flight to another for any given energy studied further suggests that the difference in the energy per nucleon spectra between the protons and the helium nuclei is not due to the transition phase but rather to the acceleration phase. This conclusion will be examined further in the next section on the acceleration process.

A few additional remarks can be made about the diffusion process. The theories referred to at the beginning of this section indicate that, both *inside* the region through which the particles diffuse and *outside* it, there is an increase of the particle flux at any given energy to a broad maximum and then a relatively slow decline. Further, the high energy particles will diffuse out more quickly with the result that the energy spectrum steepens with time—more quickly early in the event than later, when the decay phase is reached at all energies under consideration. All these features have been observed many times (References 23, 24) including the observations of this event. This event is different from some of the others in that there was most probably a moving shock wave, or magnetic bottle wall, from a previous event wherein diffusion is much slower than in the surrounding region—as already mentioned in the section "Description of the Event." Although this feature does not alter the general remarks made above, it adds sufficiently to the complexity and uncertainty of the interplanetary conditions so as to make an exact functional prediction of the change in the spectral slope extremely difficult, if not impossible. We shall, therefore, be content with saying that the general change in spectral slope noted in the "Results" section and shown in Figure 8 is not unexpected.

Acceleration

Parker (Reference 25) has shown that within the framework of the present understanding of plasma dynamics all particle acceleration mechanisms occurring outside the laboratory are reducible to the Fermi mechanism (References 26, 27, and 28), which is based on random particle collisions with magnetic inhomogeneities. The Fermi mechanism is divided into two phases, injection and acceleration. We shall begin with the former.

For acceleration to be effective, the initial particle energy must be sufficiently high so that energy losses due to interactions with ions and electrons are less than the energy gained by the Fermi process under the conditions existing in the medium. Parker (Reference 28) shows that in at least some regions the rms velocities may be such that the effective temperatures are 5×10^8 to 5×10^{10} °K and

the physical parameters are such that energy losses are completely negligible. Under these conditions there is no problem of partial ionization, since an effective temperature of only 10^7 °K is needed to completely ionize oxygen.

Since the necessary injection energy is not the same for all nuclei, an unbiased sample of the sun will be obtained at the injection point only if the rms velocity is much larger than the necessary injection velocity. In Parker's model, just mentioned, this condition is easily met for all nuclei being considered. No bias can occur in the proton to helium ratio from this cause alone because the necessary injection energy for protons and helium nuclei is the same (Reference 29).

During the acceleration phase a Fermi type of process in general leads to an integral energy spectrum of the form

$$J(>W) = \frac{C_1}{(W/W_0)^{\alpha}} , \tag{5}$$

or an equation that approaches this one in the low kinetic energy region. According to the calculation of Parker (Reference 28), α of Equation 5 is given by the expression

$$\alpha = \frac{1}{4n_0(v/c)^2} , \tag{6}$$

where n_0 is the mean number of collisions before expulsion and v is the characteristic hydromagnetic velocity. Parker's actual equation differs from Equation 5, but reduces to it for the case that $(E^2/2W_0W)$ is appreciably less than $1/\alpha$.

In the first order of the Fermi theory the energy spectrum of the particles does not depend on the charge or mass of the particle, but only on the velocity as long as the particle is charged. The experimental results obtained here, together with the previous discussion on diffusion, show however that the hydrogen nuclei have a flatter energy per nucleon spectrum than the multiply charged particles; accordingly, an explanation should be of interest. For a given velocity the rigidity, and hence the radius of curvature, will be larger for the multiply charged nuclei because of the larger mass to charge ratio. Therefore the number of collisions before escape would in general be expected to be fewer both because a particle of higher rigidity is less likely to be reflected if the disturbed centers have random sizes and because it is more likely to escape from the region. By Equation 6, then, α would be larger for the helium and medium nuclei than for protons, as observed. From this point of view, the similar energy spectra for the helium and medium nuclei is a particularly strong argument for complete ionization.

In the previous section, "Modulation and Diffusion," it was noted that the diffusion process probably acts on an initial spectrum in such a way as to yield a final spectrum that is related to the original one by a smoothly varying function of energy. It is not unreasonable, then, for an initial spectrum of the form given by Equation 5 to be changed by the diffusion process in such a way as to yield a spectrum of the same form but with a different value of α at different times in the event, as observed experimentally and shown in Figure 9.

Below 35 Mev there is a large additional group of low energy particles. Very large numbers of particles were seen at lower energies by Ogilvie et al. (Reference 9) in electronic instrumentation flown on the same flight, and satellite data have in general shown relatively large proton fluxes in the 1.5 to 15 Mev region. These particles may be a sample of the original plasma from which the high energy particles were accelerated. Although the properties of these particles probably have been changed appreciably, a mean energy corresponding to the temperatures mentioned earlier—that is, 0.05 to 5 Mev—seems reasonable on the basis of the relative number of particles at 1.5 Mev and the excess over the proposed Fermi component at 15 Mev.

If the above considerations are correct, there is some justification in first extrapolating the proton, helium, and medium nuclei energy spectra to zero by means of a straight line on a graph of flux as a function of total energy per nucleon—ignoring the additional low energy component below about 35 Mev—and then taking the extrapolated integral flux values at zero kinetic energy as representative of the relative abundances. Table 9 gives the ratios thus obtained. Notice that the ratios are the same

TABLE 9

Relative Abundances Deduced by Extrapolation of Integral Fluxes to Zero Kinetic Energy.*

Time	$\frac{\text{Hydrogen}^\dagger}{\text{Helium}}$	$\frac{\text{Hydrogen}^\dagger}{\text{Medium Nuclei}}$
1840 UT November 12, 1960	16 ± 5	$(1.0 \pm 0.3) \times 10^3$
1603 UT November 13, 1960	15 ± 5	$(1.1 \pm 0.3) \times 10^3$
Average:	16 ± 4	$(1.0 \pm 0.2) \times 10^3$

*See page 25 for a discussion of this calculation.
†The errors include the uncertainty in the extrapolation process due to experimental uncertainties only, and do not include any attempt to evaluate this method of determining relative abundances.

within errors in both flights and within the very wide limits set previously on the basis of spectroscopic evidence. The ratio thus obtained is certainly based on many *assumptions* and should not be treated as a definite conclusion; however, it appears to be worth presenting because the ratios thus obtained do not involve the very uncertain ratios deduced by spectroscopic means. Relative abundances among the multiply charged components are, of course, unaltered and need not be repeated here.

Solar Cosmic Rays and the Sun

The detection of heavy nuclei in the 1960 events of September 3 (Reference 3), November 12, and November 15 (Reference 20), together with the fact that all present evidence points toward similar relative

abundances in each case, indicates that the sun is capable of accelerating heavy ions to 10's of Mev per nucleon or more—and probably does so in every major solar event.

One of the questions of immediate interest, then, is whether or not the nuclei in solar cosmic rays reflect the relative abundances of elements comprising the sun's upper layers.

Putting aside for a moment the problem of the proton having a different charge to mass ratio from that of essentially all of the other nuclei of interest by a factor of 2, and hence a different velocity for a given rigidity, let us concentrate only on those nuclei with a charge of 2 or more. In the preceding sections, it was shown that there were good theoretical reasons for expecting the composition of the multiply charged component after the acceleration phase to reflect that of the sun when the accelerated particle fluxes of the various nuclear components are compared in the same velocity intervals.

Once accelerated, the nuclei should behave similarly because the drift and diffusion mechanisms treat all nuclei with the same Z/M factor in the same way, and the amount of material traversed in reaching the earth is certainly insignificant in terms of appreciably reducing the energy of even a 10 Mev/nucleon particle.

There is also some experimental evidence to indicate that a relatively unbiased sample of the multiply charged component of the sun has been obtained. The fact that the relative abundances of helium, carbon, oxygen, neon, and larger nuclei were the same within uncertainties *not only* in three events – two of which were in completely different regions of the sun—but *also* at two different times in the same event suggests that charges are neither favorably accelerated nor discriminated against by the acceleration process. This hypothesis is strengthened by the fact that the relative abundances obtained in this experiment are consistent with those obtained from spectroscopic measurements for those nuclei in which determinations can be made by this latter method—namely, carbon, nitrogen, oxygen, and some of the larger nuclei. Good additional evidence is provided by the similar energy spectra for helium and medium nuclei.

If the ratios obtained here are accepted as representative of the sun, then an estimate can be made of the abundance of elements such as helium and neon, which cannot be determined with any reliability by spectroscopic means because they do not emit radiation (at least not strongly) in the optical range at normal solar temperatures. As stated earlier, the measured abundances of these two elements are both within expected limits. In addition, the carbon to oxygen ratio would now be determined with relatively fine precision, compared with the ratio obtained spectroscopically.

The next logical step is to attempt to determine the abundance of hydrogen with respect to some of the others, especially helium. It has been stated previously that the protons might be expected to behave differently from the other nuclei, and their different energy spectra confirmed this suspicion; so a ratio involving protons cannot be obtained simply. To circumvent the difficulty introduced by the different charge to mass ratios, the spectroscopic value of the hydrogen to medium nuclei ratio can be used. Unfortunately there is considerable uncertainty in this value. A recent estimate based on a survey of available spectroscopic data (References 17 and 18) gave a hydrogen to medium ratio of 650, with an uncertainty probably of the order of a factor of 2. This number may then be combined with the solar helium to medium nuclei ratio obtained in this work to deduce a hydrogen to helium ratio

of 10^{+9}_{-5}. Another approach to determining this ratio, which is based only on the interpretation of the solar cosmic ray data, was discussed at the end of the preceding section on acceleration; it gave a hydrogen to helium ratio of 16 ± 4.

Comparison with Galactic Cosmic Rays

The information obtained on energetic solar particles can now be compared with the properties of galactic cosmic rays, with the aim of seeing whether or not these solar particles and ones like them from other stars can be the source of ordinary galactic cosmic rays. Until a few years ago it was generally accepted that most stars could not be important sources of cosmic rays for a number of reasons. Within the last several years it had been noted that, since the sun produced large quantities of particles whose energies were well above the injection energy needed for the Fermi theory to be operative in the galaxy (References 26 and 27), *ordinary stars* * might possibly be an important source of cosmic rays. Relatively generous estimates of particle production by the stars indicated that protons could be supplied at a rate sufficient to account for the ordinary cosmic rays, and these particles could then be accelerated in the galaxy by the Fermi method. There remained the problem of the charge composition of cosmic rays being different from normal stellar abundances, but it was thought that there might possibly be favorable acceleration of the larger nuclei.

The results of this experiment on the multiply charged components show that their abundances are just a reflection of those in the sun. There are at least four important differences within this group between solar cosmic rays and ordinary cosmic rays. Two of these — the carbon to oxygen ratio of 3:5 in solar cosmic rays compared with 3:2 in ordinary cosmic rays, and the light to medium ratio of $<1{:}100$ in solar cosmic rays compared with 1:4 in ordinary cosmic rays—may be attributed to the facts that ordinary cosmic rays have gone through a few gm/cm^2 of material wherein the light nuclei are formed by fragmentation and that there is at least an increase in the carbon to oxygen ratio. The other two differences—the different helium to medium nuclei ratios, and the different ratios between the medium nuclei and those in the charge group with $11 \leq Z \leq 18$—are only enhanced by fragmentation. The helium to medium nuclei ratio is about five times larger for the accelerated solar particles—about 68:1 as compared to 14:1 for ordinary cosmic rays, and the ratio of the medium nuclei to those in the charge group with $11 \leq Z \leq 18$ was shown in the section "Heavy Nuclei" to be four times larger for the energetic solar particles.

At galactic cosmic ray injection energies, the proton to medium ratio in solar cosmic rays is seen to be approximately 1×10^3 or larger. The proton to medium nuclei ratio for ordinary cosmic rays is about 250 for the same energy per nucleon intervals at very high energies and 100 for the same rigidity intervals. Thus the proton to medium nuclei ratio for solar cosmic rays is 4 to 10 times the ordinary cosmic ray ratio, and the difference would be slightly increased by fragmentation in interstellar matter.

*Here the term "*ordinary star*" refers to the great majority of stars with normal cosmic abundances and specifically excludes the unusual ones such as nova and supernova, which may be important cosmic ray sources.

Therefore, since the sun has abundances typical of most ordinary stars* in the respects mentioned here and since these abundances are reflected in solar cosmic rays, it seems reasonable to conclude that the *difference in the charge composition* between galactic cosmic rays and ordinary stars now remains as an objection to ordinary stars being considered as the sole primary source of galactic cosmic rays.

ACKNOWLEDGMENTS

We wish to acknowledge the whole-hearted cooperation and support of Dr. J. E. Naugle during the early phases of the solar cosmic ray experiment while he was still at Goddard Space Flight Center, and the stimulating discussions which we have had with Dr. F. B. McDonald.

We also wish to express our appreciation for the contributions of the following establishments during the entire solar beam experiment program: The U. S. Rocket Research Facility at Fort Churchill; the Canadian Defense Research Northern Laboratory; the Canadian Defense Research Telecommunications Establishment; the McMath-Hulbert Observatory; the Lockheed Solar Observatory; the Sacramento Peak Observatory; the High Altitude Observatory; the University of Hawaii Flare Patrol; the World Warning Agency, Fort Belvoir; the riometer station at Kiruna, Sweden; the riometer station at College, Alaska; and the University of Minnesota Solar Cosmic Ray Balloon Monitoring Group. We especially desire to thank the McMath-Hulbert Observatory for the early warning of the November 12 flare.

REFERENCES

1. Biswas, S., Freier, P. S., and Stein, W., "Solar Protons and α Particles from the September 3, 1960, Flares," *J. Geophys. Res.* 67(1):13-24, January 1962.
2. Ney, E. P., and Stein, W., "Solar Protons in November 1960," In: *Proc. Internat. Conf. on Cosmic Rays and the Earth Storm, Kyoto, September 1961. 11 Main Sessions,* Tokyo: Physical Society of Japan, 1962, pp. 345-353.
3. Fichtel, C. E., and Guss, D. E., "Heavy Nuclei in Solar Cosmic Rays," *Phys. Rev. Letters* 6(9):495-497, May 1, 1961.
4. Steljes, J. F., Carmichael, H., and McCracken, K. G., "Characteristics and Fine Structure of the Large Cosmic-Ray Fluctuations in November 1960," *J. Geophys. Res.* 66(5):1363-1377, May 1961.
5. Vogan, E. L., and Hartz, T. R., "Ionospheric Absorption on November 12, 1960," *Canadian J. Phys.* 39(4):630-635, April 1961.
6. Quenby, J. J., and Webber, W. R., "Cosmic Ray Cut-Off Rigidities and the Earth's Magnetic Field," *Phil. Mag.* Ser. 8, 4(37):90-113, January 1959.

*See footnote on p. 27.

7. Rothwell, P., "Magnetic Cutoff Rigidities of Charged Particles in the Earth's Field at Times of Magnetic Storms," *J. Geophys. Res.* 64(11):2026-2028, November 1959.

8. Cogger, L. L., "Magnetic Cut-Off Rigidities According to the Formulations of P. Rothwell, J. J. Quency, and W. R. Webber," Atomic Energy of Canada, Ltd., Chalk River Project, CRGP-965, AECL-1104, September 1960.

9. Ogilvie, K. W., Bryant, D. A., and Davis, L. R., "Rocket Observations of Solar Protons During the November 1960 Events; 1," *J. Geophys. Res.* 67(3):929-937, March 1962.

10. Fichtel, C. E., "The Heavy Component of the Primary Cosmic Radiation during Solar Maximum," *Nuovo Cimento* 19(6):1100-1115, March 16, 1961.

11. Fowler, P. H., and Perkins, D. H., "Measurement of Ionization in Nuclear Emulsions," *Phil. Mag.* Ser. 7, 46(377):587-610, June 1955.

12. Atkinson, J. H., and Willis, B. H., "High Energy Particle Data; II," Univ. Calif. Radiation Lab. report 2426 (rev.), Contract no. W-7405-eng-48, June 1957.

13. Heckman, H. H., Perkins, B. L., et al., "Ranges and Energy-Loss Processes of Heavy Ions in Emulsion," *Phys. Rev.* 117(2):544-556, January 15, 1960.

14. Aizu, H., Fujimoto, Y., et al., "Heavy Nuclei in the Primary Cosmic Radiation at Prince Albert, Canada; I. Carbon, Nitrogen, and Oxygen," *Phys. Rev.* 116(2):436-444, October 15, 1959.

15. Tamai, E., "Heavy Nuclei in the Primary Cosmic Rays over Minnesota," *Phys. Rev.* 117(5):1345-1351, March 1960.

16. Davis, L. R., Fichtel, C. E., et al., "Rocket Observations of Solar Protons on September 3, 1960," *Phys. Rev. Letters* 6(9):492-495, May 1, 1961.

17. Goldberg, L., Muller, E. A., and Aller, L. H., "The Abundances of the Elements in the Solar Atmosphere," *Astrophys. J.* 5(suppl. Ser. 45):1-138, November 1960.

18. Aller, L. H., "The Abundance of the Elements," New York: Interscience Publ., 1961.

19. Suess, H. E., and Urey, H. C., "Abundance of the Elements," *Rev. Modern Phys.* 28(1):53-74, January 1956.

20. Waddington, C. J., "The Composition of the Primary Cosmic Radiation," In: *"Progress in Nuclear Physics"* 8:1-45, New York: Pergamon Press, 1960.

21. Parker, E. N., "Modulation of Primary Cosmic-Ray Intensity," *Phys. Rev.* 103(5):1518-1533, September 1, 1956.

22. Simpson, J. A., "Solar Flare Cosmic Rays and Their Propagation," *Nuovo Cimento* 8, Suppl. 10(2):133-160, 1958.

23. Webber, W. R., "Time Variations of Low Energy Cosmic Rays During the Recent Solar Cycles," In: *Progress in Elementary Particles and Cosmic Ray Physics*, ed. by J. G. Wilson and S. A. Wouthuysen, Amsterdam: North-Holland Publ. Co., Vol. 6, 1962 (In Press).

24. Winckler, J. R., Bhavsar, P. D., et al., "Delayed Propagation of Solar Cosmic Rays on September 3, 1960," *Phys. Rev. Letters* 6(9):488-491, May 1, 1961.

25. Parker, E. N., "Origin and Dynamics of Cosmic Rays," *Phys. Rev.* 109(4):1328-1344, February 15, 1958.

26. Fermi, E., "On the Origin of the Cosmic Radiation," *Phys. Rev.* 75(8):1169-1174, April 15, 1949.

27. Fermi, E., "Galactic Magnetic Fields and the Origin of Cosmic Radiation," *Astrophys. J.* 119(1):1-6, January 1954.

28. Parker, E. N., "Acceleration of Cosmic Rays in Solar Flares," *Phys. Rev.* 107(3):830-836, August 1, 1957.

29. Hayakawa, S., and Kitao, K., "Energy Loss of a Charged Particle Traversing Ionized Gas and Injection Energies of Cosmic Rays," *Progr. Theoret. Phys.* 16(2):139-148, August 1956.